

See discussions, stats, and author profiles for this publication at: <https://www.researchgate.net/publication/221226043>

# Color Enhancement in a High Dynamic Range Environment

Conference Paper *in* Proceedings of SPIE - The International Society for Optical Engineering · February 2009

DOI: 10.1117/12.805573 · Source: DBLP

---

CITATIONS

2

---

READS

39

## 3 authors:



[S. Marsi](#)

Università degli Studi di Trieste

48 PUBLICATIONS 451 CITATIONS

[SEE PROFILE](#)



[Alfredo Restrepo](#)

Los Andes University (Colombia)

59 PUBLICATIONS 529 CITATIONS

[SEE PROFILE](#)



[Gabriele Guarnieri](#)

Università degli Studi di Trieste

15 PUBLICATIONS 82 CITATIONS

[SEE PROFILE](#)

# Color Enhancement in a High Dynamic Range Environment

Stefano Marsi, Alfredo Restrepo and Gabriele Guarnieri

IPL - DEEI - University of Trieste, Via Valerio 10, 34127 Trieste, Italy

## ABSTRACT

We present techniques for the processing of color, high-dynamic luminance images of a type aiming for objectivity and also of a type aiming for aesthetic improvement. In the first case we start with camera raw data, propose a variant white balance, darken very light spots and lighten very dark spots. In the second case we use color spaces of the type hue-saturation-luminance; we propose a hue processing method inspired in the Bezold-Brucke effect as well as a luminance-dependant displacement of color saturation.

**Keywords:** High dynamic, color enhancement, white balance, hsv, rgb

## 1. Introduction

When processing images with a high dynamics luminance one may aim either for objectivity or for aesthetics. The human visual system (HVS) has the ability to perceive the *true color* of objects regardless of the spectral contents of the illuminant, within bounds.<sup>1</sup> In many cases, e.g. in computer vision and in product inspection, we would like to replicate this ability; however, when we visualize on a monitor or print a hardcopy of an image, we must deal with the limited dynamic range of the acquisition and, mainly, of the visualization devices. The result is often a poor picture where overexposed or underexposed zones appear, particularly if it has been acquired under critical illumination conditions, such as backlighting or intense light sources together with dark environments. Moreover, the colors will appear different from our original perception, since they depend on the different spectra of the lighting conditions, which change for instance between daylight and fluorescent or incandescent light.<sup>4</sup>

Current digital cameras use a data bus of more than 12 bits, good enough for many applications, even under quite critical conditions. Nevertheless, a bottleneck remains at the reproduction device; high dynamic monitors<sup>6</sup> are still at a prototype stage, they are costly and power-hungry and their usage is limited to controlled environments, e.g. in scarcely illuminated or a dark rooms, without light sources incident on the screen.

In this paper we present an algorithm for the processing of images acquired under critical high dynamic conditions; it 'squeezes' the image to fit the range of the visualization device, whether HDR or not. Moreover, the algorithm implements a color balancing method aimed to give the same visual impression the photographer had when he looked at the original scene. The algorithm is given in Section 2. The proposed algorithm has as input the so-called raw data of the camera rather than the RGB image used for visualization. In fact the conversion from raw to RGB introduces some nonlinearities, such as gamma correction and, more importantly, some signal saturations are typically executed in order to avoid the presence of out-of-range data. In the camera, the raw data are more robust and include more information than the RGB data. The proposed novel aspects are thus threefold. First we operate on the raw image data; secondly, dark parts of the scene are made brighter, and bright parts are darkened (while typical processing techniques such as<sup>16</sup> only do the former) and, thirdly, we introduce a method for automatic, space-variant white balance.

The algorithm just mentioned aims for objectivity. We consider as well other aspects regarding chromaticity under high dynamic range conditions. We propose tools that can be used for enhancing the aesthetics of such images. For this, we use one of the color spaces derived from the RGB representation, such as HSV, HSL or HSI, where the chromatic aspects of hue and saturation are made explicit. A drawback of these color spaces

---

<sup>a</sup>E-mail:arestrepo@units.it, Telephone: +39.040.5587140 (A. Restrepo is currently on leave from Dpt. Ing. Electr. y Electr., Universidad de los Andes, Bogota, Colombia; arestrep@uniandes.edu.co)

<sup>c</sup>E-mail: marsi@units.it, Telephone: +39.040.5582542

is that the (saturation, luminance) pair does not live in a region as simple as the square  $[0, 1] \times [0, 1]$ , but in regions with more elaborate shapes. The fact that the hue is a circular variable, on the other hand presents more standard challenges<sup>19, 20</sup>.

## 2. Description of the algorithm

We present an algorithm designed to improve the visual quality of an image acquired under critical illumination conditions that may include a high-dynamics luminance, the presence of several illumination sources or the presence of very bright or radiant surfaces.

### Critical illumination conditions

A luminance component with high dynamics commonly results when imaging nature; in particular, when some parts of the scene are abundantly illuminated e.g. by direct sunlight while other areas are in the shadow and are illuminated only indirectly with reflected light or with filtered light (e.g. by the leaves of a tree). This presents the photographer with a common challenge: as is well known, the preservation of the details in one kind of area compromise the visibility in the other one; thus, for instance, if the dark area is well exposed, the brighter zones will be overexposed; otherwise, if the exposition is tuned for a good resolution in the brighter area then the darker zones result underexposed.

Likewise, the presence of several, spectrally different, illumination sources presents problems for the reproduction of color in a camera-display system; specifically when using white balance techniques. Even though metamerism can be created/destroyed as a result of a change of the spectral conditions of the illuminant (a painter that works at night under a light bulb is likely to see his work differently when observed under sunlight) we nevertheless identify the properties of the surfaces of objects rather independently of the spectral contents of the illuminant and we say that (under photopic conditions) we perceive the *correct colors of objects* either at day or night. We perceive the colors (of objects) in a rather intrinsic fashion, quite independently from the spectral contents of the illuminant; thus, a piece of white paper is perceived as *white* both under direct sunlight and under an incandescent tungsten lamp light. Even if we adapt to the spectral contents of the illuminant and do not seem to notice things yellow, when the same scene is illuminated by direct sunlight in one case and by incandescent light in the other, and corresponding images are acquired by a camera and afterwards represented on a monitor or printed on a hardcopy, the results obtained for different lighting conditions can be quite dissimilar: typically the images of scenes illuminated with tungsten lamps are yellower than those illuminated with direct sunlight. Typically, images with whites are preferred and the resulting problem is solved by the use of so-called "white balancing" processing algorithms<sup>3, 8, 9, 10</sup>; such algorithms have been developed to compensate this behavior. Unfortunately typically the solution proposed is based on the assumption that the entire image is illuminated by the same light source, however, unfortunately, this assumption can, in some critical cases, fail. There can indeed be conditions where different light sources illuminate the scene, for example when the scene includes both indoors and outdoors views; in such a case, the standard solution can create erroneous compensations at parts of the image producing annoying artifacts. Finally, the presence of very bright or radiant surfaces in the scene may result in a saturated response of the camera sensors producing data that do not represent adequately the real physical stimulus.

### Algorithm overview

To deal with the critical conditions mentioned above we have developed the algorithm depicted in Fig. 1. We initially briefly describe the general behavior of the algorithm, a more complete explanation of the various sub-blocks is given further down.

The input to the system is given by the *raw data* channels at the camera sensors, called here LMS (like the cones in the retina). Such data are quite different from the more commonly used RGB components. They carry more information than the corresponding RGB data, maintaining a complete color description and the full dynamics of the signal.

Broadly speaking, the algorithm implements a *spatially-dependent automatic-compensation of the camera exposure*, i.e. a variant compensation, weighted by the luminance at the different spots of the image. After the

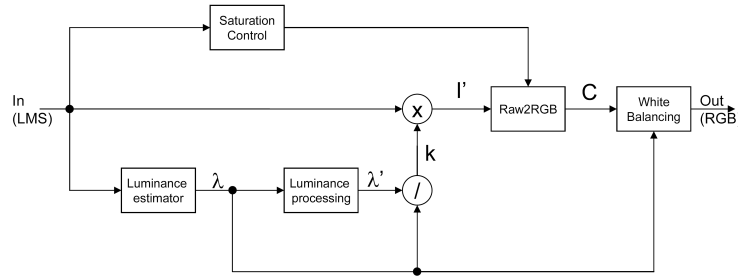


Figure 1. Block diagram of the proposed algorithm

evaluation, pixel by pixel, of the mean of the three raw input channels lms, a suitable edge preserving smoothing (bilateral) filter<sup>7</sup> is used to estimate the intensity of the luminance  $\lambda$  at different zones in the image. Using this information the LMS data are multiplied by a suitable coefficient  $k$  which takes different values in the different parts of the image accordingly to the  $\lambda$  value: in dark areas  $k$  is chosen greater than one to perform an increment of the exposition of the camera parameters; meanwhile, at brighter spots,  $k$  can be chosen lower than one to avoid possible saturation and over-exposition effects. This process is repeated for each of the LMS components, using the same value of  $k$ . As a second step, the algorithm converts the raw data into a suitable RGB space for visualization purposes. However, since at the first stage the algorithm has modified the dynamics of the image, certain color artifacts may appear in the areas where the original color information was corrupted, due to the saturation of one or more of the input sensors. To check for this event, an appropriate block analyzes the spots where a sensor saturated (that is, took its maximum possible value) and performs a suitable correction when converting to RGB, giving an achromatic color to the spot. In a third stage, the algorithm implements the white balancing control that permits an image with "natural" colors, compensating the illumination conditions of the scene. For natural images (i.e. those arising from physical scenes), it often happens that the illuminant is not the same for the entire image, an obvious example being an indoor and an outdoor views, present in the same scene. To achieve a good result it is important to be able to discriminate which parts of the image are illuminated by the various light sources and to use this information to achieve a correct white compensation (compare with<sup>18</sup>). To deal with this problem we have developed a simple but quite effective solution where the white balancing algorithm is controlled, by the luminance estimation  $\lambda$ .

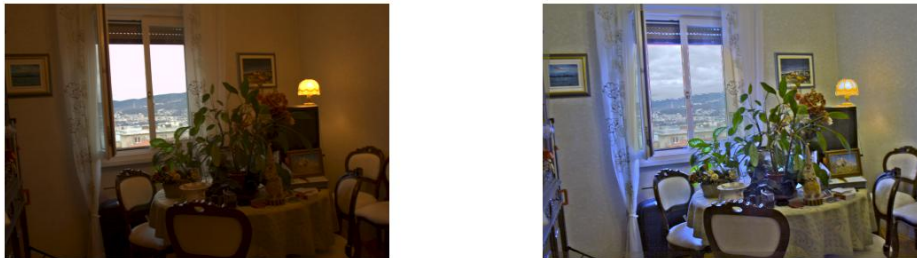


Figure 2. Algorithm performance: on the left, RGB version of input image without any processing; on the right, the resulting image after the application of the proposed algorithm.

## Input data

As mentioned, the input to the algorithm are not the canonical RGB components, but the raw data LMS from the camera sensor. As with the first cameras, current color cameras emulate the human visual system. They employ three color filters inserted before the sensors, often assembled in a structure called a "Bayer Pattern". These filters have quite large bandwidths that differ from one camera to the other, and actually do not closely follow the response curves of the *primaries* (e.g. RGB or CMY) used. In fact, while the LMS filters of the

camera spectrally characterize the input, suitably weighted primaries, taking advantage of metamerism and the tridimensionality of color, allow us to perceive the result in the same way as the original stimulus, even if spectrally different.

The transformation from the LMS raw domain to the RGB image depends on the filters used in the camera and on the primaries adopted by the visualization device. Note that while for monitor devices a standard has been recently adopted (sRGB), for the camera, we still far away from adopting a standard, and each company engineers its own products with different characteristics; for instance, some cameras use filters with spectral responses which can be interpreted as cyan magenta and yellow instead of red green and blue; however, also in the case of red green and blue filters, their spectral response is not standard and in each case, the transformation strictly depends on the spectral responses of the color filters used.

This step of converting the acquired LMS raw image to an RGB image is not always an injective transformation and an observation is pertinent: in some cases a single RGB image corresponds to different LMS input data. This is due to the fact that the RGB space, limited in the canonical range  $[0,1]$  does not allow for negative values nor for values larger than one; moreover, 3 channels are not sufficient to recreate all the natural colors. However, all such information is present in the raw data and could be usefully processed. To deal with the raw information in the algorithm allows to process the data without the lost of information that the use of RGB may comport. Moreover it should be noted that the transformation from the raw data to RGB is a non-linear one since it involves gamma adjustments; thus, to emulate a different exposure in the raw data is quite simple and can be easily managed just by multiplying the raw data by a different gain factor; the same process, applied in the RGB domain produces a completely different result. Figs. 5.a shows how the raw native domain lms cube  $[0,1]^3$  is mapped to the RGB domain. Note that to represent the entire input range we should admit values outside RGB cube  $[0,1]^3$ . The fact that the image is not a parallelepiped makes it patent the non linear nature of the transformation. However it is also important to notice that (due to the overlapping nature of the lms responses) in the raw image, not every position in the lms  $[0,1]^3$  cube can be actually reached; thus, for real images, the domain of the not representable stimulus is considerable limited with respect to the one represented in the figure.

The difference between applying the luminance control at the LMS rather than the RGB level is depicted in Figs. 3.b,c. It should be noted that in the first case a part of the information (like the clouds outside the window) are totally absent. Notwithstanding both images present a reddish dominant due to the tungsten lamp illumination (which will be eventually compensated by the white balancing algorithm), Fig. 3.b looks unnatural and appears too saturated.



Figure 3. Example of processing in different color spaces: On the left, transformation from the native raw space to RGB space. On the center the result when the luminance control is done on the RGB space. On the right the control as performed on the raw LMS space.

### Luminance estimation

The illuminant is a feature that for natural images typically changes piecewise quite smoothly; thus, it is generally accepted to model it as a low-frequency spatial signal. However, abrupt transitions sometimes appear at points where there is an environmental variation such as at the boundary of a window in a room through which the outdoors is seen during day time. Both at the inside and at the outside regions, the illumination can be considered quite constant, with some smooth variation; but at the transition boundary, the illumination presents

of course a very abrupt transition. The solution to model such a peculiar signal can be found in the usage of an edge preserving smoothing filter. In the proposed algorithm we have employed a modified version of the bilateral filter. The bilateral filter, introduced by Tomasi and Manduchi ??, is substantially a nonlinear FIR filter, with signal-dependent coefficients. As in an FIR filter, the output is computed by a weighted average of the pixels in a neighborhood, and the edge-preserving effect is achieved by giving a smaller weight to the pixels the value of which differs substantially from the value of the pixel in the middle of the filter's mask. In our case, we have used just two weights for all the pixels, one and zero, according to the following equations:

$$h(m_1, n_1) = 1, \text{ if } kx(m, n) < |x(m + m_1, n + n_1) - x(m, n)| < \frac{1}{k}x(m, n); h(m_1, n_1) = 0, \text{ otherwise.}$$

$$y(m, n) = \frac{\sum_{m_1=-d}^d \sum_{n_1=-d}^d h(m_1, n_1)x(m+m_1, n+n_1)}{\sum_{m_1=-d}^d \sum_{n_1=-d}^d h(m_1, n_1)}$$

Where  $d$  defines the size of the mask and  $k \in [0, 1]$  tunes the edge preserving behavior. If  $k$  tends to zero, the edge preserving effect is turned off while the higher the  $k$  the closer a pixel must be to the central one to have an effect at the filter output. It should be noted that this edge preserving effect depends both on the amplitude of the edge itself and on the intensity of the central pixel; thus, the algorithm, according to Weber's law, preserves better the edges in the dark areas than in the lighter ones. The edge preserving effect is fundamental for the pleasantness of the final result; otherwise, very annoying haloes appear. An comparison example of the luminance estimation with and without this edge preserving strategy is depicted in Fig. 4 together with the final result obtained with these settings.

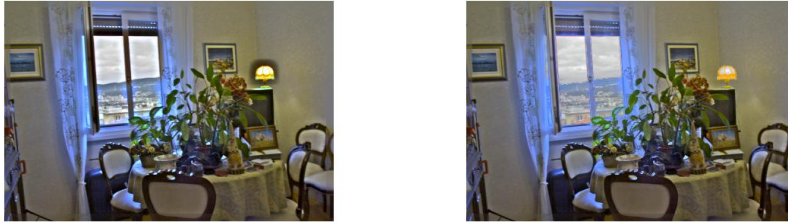


Figure 4. Effectiveness of the edge preserving strategy: the result without edge-preserving on the left, with edge preserving on the right.

### The luminance processing control

To obtain a good exposure in a snapshot, the photographer typically acts on the exposure controls, the iris and the time shutter, to get the right stimuli at the sensor. However, if the scene contains bright spots as well as poorly illuminated zones, usually a compromise must be made, since the camera cannot control separately such parameters at different zones in the image.

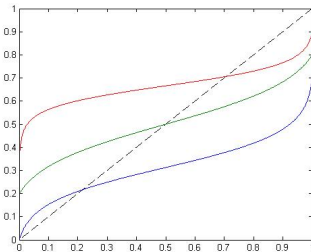


Figure 5. Three examples of the non linear function used to control the luminance.

On the contrary, the algorithm we propose is based on the idea of emulating exposure controls that can vary across the different parts of the image. The parameter that control the exposure is the gain factor  $k$  which

depends on the estimated luminance at different areas of the image, as applied to each of the raw sensor channels LMS. If  $\lambda$  is the estimated luminance, we first obtain an  $\lambda'$  via a non linear mapping function with a shape like those depicted in Fig. 5 where it is possible control the slope and the gain for values of  $\lambda$  near 0 and near 1. The function is a scaled version of an inverse sigmoid function and, with its shape, it helps to increase the exposure at the dark areas and to reduce it at the brighter ones. Eventually, the appropriate gain control is obtained from the ratio between  $\lambda'$  and  $\lambda$ .

### Raw to RGB conversion and saturation control

The raw data LMS represent the image at the acquisition level, i.e. they are the data at the output of the camera sensors. On the other hand, the RGB signals represent the image at the visualization level; they, coarsely speaking, indicate the weights to apply to three the red, green and blue primaries; they are usually but not always (e.g. LCD displays) quite monochromatic light sources. Combined, they provide a reconstruction that results in an image that looks to the eye practically identical to the original stimulus scene. The conversion from one space to the other is made usually in a two-step process. First, a linear conversion from Raw to XYZ (the standard tristimulus space) is made; this is a linear transformation that depends on the camera and on the spectral responses of the three color filters employed. Secondly, the conversion from XYZ to RGB is a quite standard nonlinear transformation involving a "gamma compensation" that mainly depends on the particular RGB space. In fact, there are several RGB spaces, depending on the particular set of primaries adopted. This two-step transformations transforms the data from raw to RGB. However, since the transformation can produce data outside the required RGB range  $[0,1]$ , a saturation at 0 or at 1 of the RGB level occurs respectively for negative values and for values larger than one. As Fig. 3 makes evident, it is far better to use this transformation after the luminance control process. However, in a few cases, undesired artifacts can result. In fact, if the original raw data became saturated at some point (i.e. the stimulus was so intense as to make one or more of the channels LMS saturate) the resulting RGB interpretation is corrupted and incomplete, probably generating a saturated white; however, if this corrupted data are previously scaled by the luminance control process, it will enter in the visible range, but with a color information incorrect and the result will be a uncorrected highlights color. To avoid this undesired behavior a simple control is implemented; just before the raw to RGB transformation, a check is made if the original data present some saturation, in which case, the color information is discarded and transformed to achromatic data. An example of the effectiveness of this approach is shown in Fig. 6. At the left, the image is obtained without the saturation control; it can be noted the sky appears magenta: the original data at this spot present a significant saturation on the raw data so that after the luminance control and the transformation to RGB this corruption produces an uncorrected color. On the right, the saturation control transforms these highlighted areas to achromatic, obtaining a more natural effect.

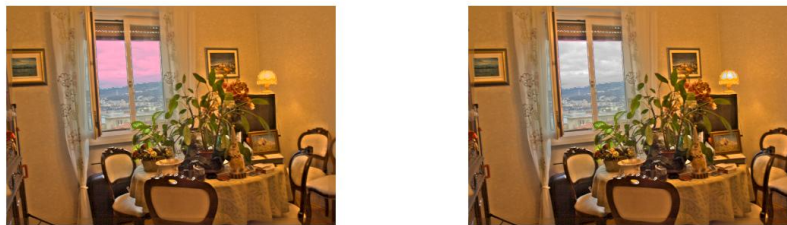


Figure 6. Effectiveness of adopting the control scheme on the saturation: On the left, the result without the control; on the right, with the control active.

### The white balancing algorithm

It is well known that photographs often appear different from the real world we perceive, depending on the illumination under which the image is taken. Different light sources have different spectral characteristics, thus requiring an adjustment of the captured image for the scene illuminant to recover its true coloration. However, the camera cannot judge the actual subject color, nor can it estimate the spectrum of the illuminant. Therefore, so-called white balancing solutions are applied; they aim to adjust the image automatically, for instance by finding

whitish areas to set the parameters for balancing the colors in the remaining parts of the image. Existing popular solutions use different concepts, such as the multi-scale clustering approach,<sup>23</sup> the grey-world assumption,<sup>24</sup> and the Retinex theory.<sup>25</sup> Unfortunately, these solutions fail to take into consideration the local image characteristics, thus often compromising the final image quality. In fact, in some critical cases the illuminant of the image is not the same for the entire image and thus the white balancing should be distinct in the different illuminated areas. For instance, the image we have adopted to test the algorithm presents both indoor and outdoor views; obviously, the illuminant is different for these two cases. Following this strategy we have developed a simple but effective way to discriminate between the different light sources, based on the luminance estimation. The main idea is to discriminate between the highlights and the zone in the shadow, apply separately on them the white balancing algorithm and then merge the results into a final image. More in detail: Starting from the luminance estimation  $L(m,n)$  we apply on it a suitable non-linear function as the one depicted in Fig. 7.a to obtain a mask  $M(m,n)$ . An example of such a mask is depicted in Fig. 7.b. The adopted function is a simple linear function with two tuning saturation thresholds  $t_1$  and  $t_2$ . If the input datum is under the lower threshold  $t_1$ , the output is set to zero; if it is larger than  $t_2$ , the result is saturated to one, and between  $t_1$  and  $t_2$ , a constant slope is used. The values of  $t_1$  and  $t_2$  can be suitably modified depending by the input image.

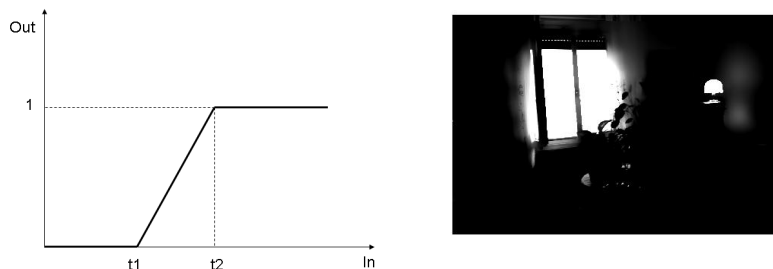


Figure 7. On the left the nonlinear function used in the definition of the mask  $M(m,n)$ ; on the right, an example of the mask.

$$M(m, n) = F(L(m, n))$$

Using this mask the image to balance  $C(m, n)$  is splitted into two different images  $C_1(m, n)$  and  $C_2(m, n)$  given by  $C_1(m, n) = C(m, n)M(m, n)$  and  $C_2(m, n) = C(m, n)(1 - M(m, n))$ , and thus  $C_1(m, n) + C_2(m, n) = C(m, n)$

On each of  $C_1$  and  $C_2$ , a standard white balancing algorithm based on the gray world assumption, like the one proposed in,<sup>7</sup> is accomplished: calling the three RGB coordinate of the image to process and assuming are the corresponding coordinate of the final result. Since the wavelength of the G color band is close to the peak of the human luminance frequency response, the algorithm keeps the input G components unchanged (i.e. ) and adjusts only the R and B channels using the adaptive gains and as follows: and , where

$$\alpha = \frac{\bar{G}(m, n)}{\bar{R}(m, n)} \text{ and } \beta = \frac{\bar{G}(m, n)}{\bar{B}(m, n)}$$

and  $\bar{R}(m, n)$  ,  $\bar{G}(m, n)$  and  $\bar{B}(m, n)$  represent the mean values of the corresponding R, G, B signals; after this process on both  $C_1(m, n)$  and  $C_2(m, n)$  we obtain two new images  $C'_1(m, n)$  and  $C'_2(m, n)$ . Eventually the final image is obtained as

$$Out(m, n) = M(m, n)C'_1(m, n) + (1 - M(m, n))C'_2(m, n)$$

In Fig. 8, two possible results are compared: on the left, white balancing is performed on the entire image without any subdivision into low- and high-luminance areas, while on the right the proposed white balancing algorithm has been applied. As can be noted, in both cases the reddish dominant hue has been compensated but, in the first case, global white balance leads to uncorrect colors for the outdoors scene.

### 3. Chromatic effects based on changes of the hue and saturation components

We present a set of tools for the processing of high dynamic images that are intended to improve their aesthetics, if not their realism. We consider dependencies on the luminance  $\lambda$  of the chromatic aspects of saturation  $\sigma$  and



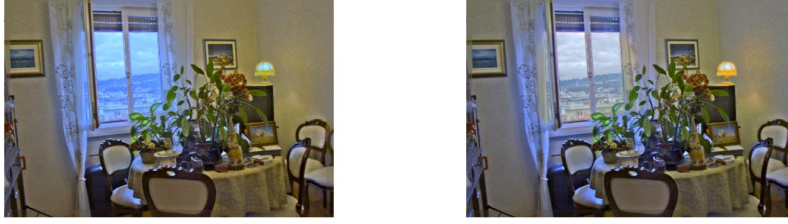


Figure 8. wbglobalweighted

hue  $\eta$ . The saturation of a color tells us how different it is from an achromatic color; since in RGB color systems achromatic colors fall along the line  $R = G = B$  of the RGB cube, a large value of the range of the triple  $(R, G, B)$  is evidence of large color saturation. Color systems that make explicit color saturation weight this range by a measure of the luminance of the pixel.

From a sensorial point of view, Bezold-Brücke effect predicts a shift of hues that, if extended to *related colors*, predicts as well a loss of saturation due to a clustering of hues. BB effect is for photopic vision and for unrelated colors, i.e. the color of a surface patch set against a dark background, similar to the case of the blue of the sea or the sky or the green of a meadow, when they occupy pretty much the whole field of view. Also, we find it to be an empirical fact that in natural images color saturation tends to depend inversely on luminance.

### Hue-Saturation-Luminance color systems

The HSV (the *hexcone* model), HSL and HSI color representation systems define their variates in terms of the RGB variables. Generically, we call them  $\eta\sigma\lambda$  spaces. Even though there seems to be no agreement as to the precise formulas, we use<sup>22</sup> for the luminance component  $\lambda$ ,  $V = \max$ ,  $I = (R+G+B)/3$ ,  $L = (\max+\min)/2$ , respectively, for the HSV, HSI and HSL systems; where where  $\max := \max(R, G, B)$ ;  $\min := \min(R, G, B)$ ; also, we denote the midrange as  $\mu := 0.5(\max+\min)$  and the range as  $\rho = \max-\min$ .

For the saturation component  $\sigma$ , we use  $S = 0$ , if  $\max=0$ ;  $\frac{\max-\min}{\max}$ , if  $\max \neq 0$ ;  $S = 1 - \frac{\min}{I}$ ;  $S = 0$ , if  $\rho=0$ ;  $\frac{\rho}{2\mu}$ , if  $\mu \leq 0.5$ ;  $\frac{\rho}{2(1-\mu)}$ , if  $\mu > 0.5$ ; respectively, for the HSV, HSI and HSL systems.

Finally, for the hue component  $\eta$ , we use  $H = \frac{1}{6} \frac{G-B}{\rho}$  if  $\max=R$ ,  $H = \frac{1}{6} \frac{B-R}{\rho}$  if  $\max=G$  and  $H = \frac{1}{6} \frac{R-G}{\rho}$  if  $\max=B$ , for the HSV model.  $H = 60 * \frac{g-b}{\rho}$ , if  $\max = R$ ;  $H = 60 * \frac{b-r}{\rho} + 120$ ; if  $\max = G$ ;  $H = 60 * \frac{r-g}{\rho} + 240$ , if  $\max = B$ ; for the HSL system, and  $H = \frac{2\pi-\phi}{2\pi}$  if  $B > G$ , and  $H = \frac{\phi}{2\pi}$  if  $B \leq G$ , where  $\phi = \arccos \frac{2R-G-B}{\sqrt{R^2+G^2+B^2-RC-GB-RB}}$ , for the HSI model.

### On the relationship between luminance and color saturation in photographs

The term *color saturation* has the sense of the color-vision concept (e.g. 'Colorfulness of a area judged in proportion to its brightness'<sup>1</sup> ; or: 'Saturation is the attribute of a visual sensation which permits a judgement to be made of the degree to which a chromatic stimulus differs from an achromatic stimulus regardless of their brightness'<sup>21</sup>), and also, the even more specialized sense of a formula that intends to make explicit this sensory aspect in a given color space.

Even though, under photopic conditions, 'a color stimulus of a given chromaticity exhibits approximately a constant saturation for all luminance levels, except when brightness is very high'<sup>1</sup> , we find that on many photographs, there seems to be a loss of color saturation with luminance; see scatter plots in Figs. 11 and 12. Whether there are physical reasons for this, or it is due to a limitation of the color space, or due to reasons steaming from the physics of the image and properties of the human visual system in the processing of high dynamic images, we balance this tendency by decreasing color saturation at low luminances, and viceversa.

The image of the RGB cube  $[0, 1]^3$  under one of the  $\eta\sigma\lambda$  transforms determines the possible values the pair  $(\sigma, \lambda)$  (i.e. saturation, luminance) can take which in general depends on the value of  $\eta$ . Thus, the relationship

between saturation and luminance is also limited by the boundary on the image set of the RGB cube. In a sense, the processing of the  $\eta\sigma\lambda$  components should be made on the basis of *flows* defined on such image set. It often happens that a correction of color saturation does not respect the boundary of this image set, the saturation being then truncated by the computer with the effect of unnatural blocky artifacts in the resulting RGB image.

Assume that the pixels in the image have been classified (either on a pixelwise basis or with a region growing algorithm with user-given start points<sup>18</sup>) as having one of three types of luminance: high (in the pixelwise case,  $> 0.7$ ), intermediate (in the pixelwise case between 0.3 and 0.7) or low ( $< 0.3$ , in the pixelwise case). Since, empirically, the saturation tends to be an inverse function of the luminance, in the case of low luminance we apply gamma correction to the saturation with an exponent larger than one, decreasing the saturation while for high luminances, the exponent  $\gamma$  is smaller than one, increasing the saturation. See Fig. 9.c. Also, since the range of the triple (R, G, B) is likely to be reduced as an effect the resulting clustering of hues, BB effect is related to a desaturation of colors with high levels of radiance.

### Uses of artificial Bezold-Brücke (BB) effects

The Bezold-Brücke (BB for short) effect (which predicts a yellowing of oranges and cetrines and a shift towards blue of cyans and purples with an increase of the intensity of the illuminant), if extrapolated to related colors, tends to polarize the chromaticity along Hering's Yellow-Blue dimension. A cyan sea becomes bluer and a cetrine grass becomes yellower, and maybe unconsciously, we expect this to happen, e.g. at noon under a blue sky. A decrement of the intensity of the light on the other hand, places colors more and more along the red-green axis and we get those nice typical colors of christmas decorations. Goethe pointed out the close relationship that exists between yellow and brightness on the one hand and between blue and darkness on the other. A radiant blue is pretty conspicuous at night but not so much in daytime.

For the processing of color images we define a *light Bezold-Brücke shift* as a continuous map from the hue circle to itself that leaves invariant the hues red, green, blue and yellow and that makes yellower oranges and cetrines and makes bluer violets and cyans. Similarly, a *dark Bezold-Brücke shift* is a map that leaves invariant the 4 hues red, green, blue and yellow and that makes greener cyans and cetrines while making redder violets and oranges. See Figs. 9.a,b. For example, consider the following, used in the processing of teh image in Fig. 13. Initially, let  $g : [-\frac{\pi}{2}, \frac{\pi}{2}] \rightarrow [-\frac{\pi}{2}, \frac{\pi}{2}]$  is given by  $g(x) = 0.5(2x/\pi)^2 + 0.5(2x/\pi)$  if  $x > 0$  and  $g(x) = -0.5(2x/\pi)^2 + 0.5(2x/\pi)$  if  $x < 0$

Now, for a dark BB shift, let  $f : S^1 \rightarrow S^1$  given by  $f(x) = g(x) + x$  for  $-\frac{\pi}{2} < x < \frac{\pi}{2}$   $f(x) = g(x - \pi) + x$  for  $\frac{\pi}{2} < x < \frac{3\pi}{2}$  while for a light BB shift, let  $f : S^1 \rightarrow S^1$  given by  $f(x) = g(x - \pi/2) + x$  for  $0 < x < \pi$   $f(x) = g(x - 3\pi/2) + x$  for  $\pi < x < 2\pi$

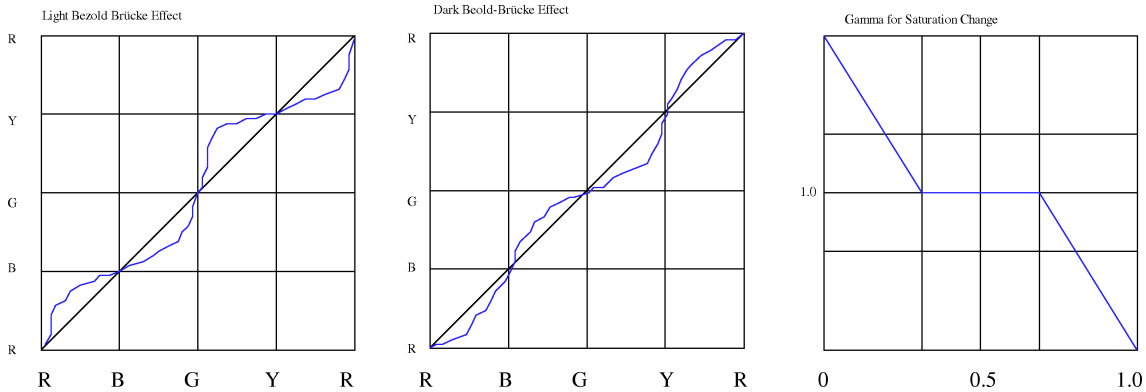


Figure 9. BB dark, light; saturation

## 4. Conclusion

Due to the limitations of the dynamic range of cameras and, mainly, of visualization devices, the development of tools for a suitable visualization of images from high dynamics scenes is an important topic of research. Our



Figure 10. Mercado.

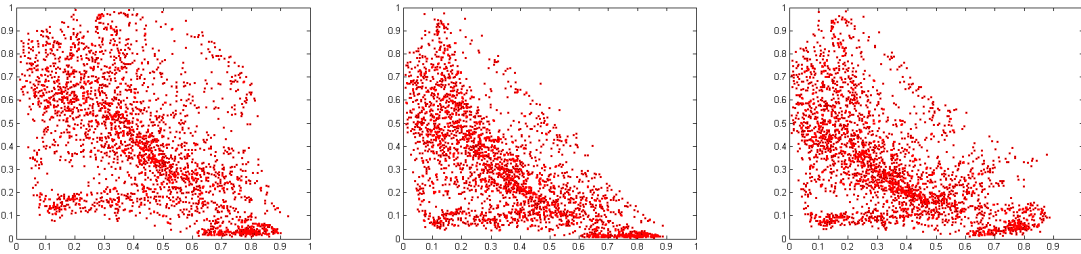


Figure 11. Sat.vs.Lum HSV, HSI, HSL; corresponding to the image Mercado.

grain of sand consists of the use of raw data that permits access to a richer source of information than camera RGB data, the use of a variant white balance and tools that lighten dark areas as well as darken light areas. In a related vein, we have developed tools for hue and color saturation processing related to the ways we perceive hues under high radiance conditions and to the way, as observed, color saturation is related to luminance in camera images. Another goal might be to have an image taken under noon light look like an image taken at dusk, or viceversa; this could be useful also in the movies industry. Two things should be taken into account; what the effects on perception are for simultaneous strong and weak light intensity and what the effects are on the photo image one gets from a determined type of camera. The first tells us what we expect and should be used to correct the second.

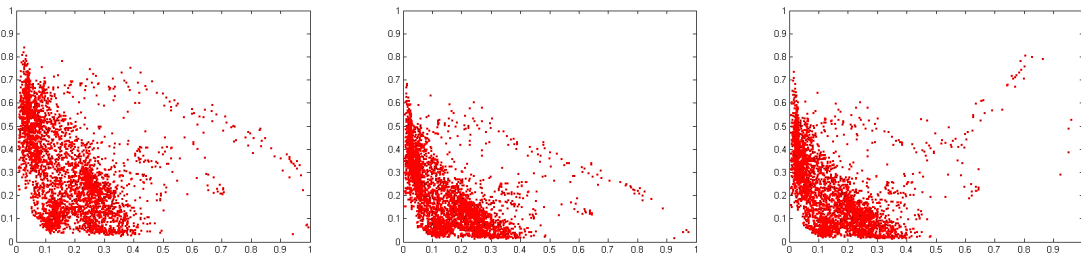


Figure 12. Losana; Sat.vs.Lum HSV, HSI, HSL; corresponding to the image on the left in Fig. 13



Figure 13. Losana; Luminance dependant processing of luminance, saturation and hue in HSV system; valinf=0.5, valsup=0.8, a=1.1, gs1=2, gs2=0.5, gv1=0.7, gv2=5

## REFERENCES

1. Fairchild, M.D. [Color Appearance Models], Addison Wesley, (1998).
2. Agar, A.U. and Allebach, J.P. "Model-based color halftoning using direct binary search Image Processing," *IEEE Transactions on Image Processing* 14(12), 1945-1959. (2005)
3. Finlayson, G.D., Drew, M.S. and Funt, B.V., "Diagonal transforms suffice for color constancy," *Proc. Fourth International Conference on Computer Vision*, 164 - 171 (1993).
4. van de Weijer, J., Gevers, T., Gijssenij, A., "Edge-Based Color Constancy" *IEEE Transactions on Image Processing*, 16(9)2207-2214 (2007).
5. Ledda, P., Chalmers, A., Seetzen, H., "HDR displays: a validation against reality" *IEEE International Conference on Systems, Man and Cybernetics*, 2004. 3 2777-2782 (2004)
6. Hiroaki S., Hideyuki K., Shuichi K., Jun S., Hideki T., "Wide Color Gamut Displays Using LED Backlight" *Conference Signal Processing Circuits Industry Applications, 41st IAS Annual Meeting. Conference Record of the 2006 IEEE* 2 686-689 (2006)
7. Guarnieri, G., Marsi, S., Ramponi, G., "Fast bilateral filter for edge-preserving smoothing" *Electronics Letters*, 42 (7) 396-397 (2006)
8. Chong, H.Y., Gortler, S.J., Zickler, T., "The von Kries Hypothesis and a Basis for Color Constancy," *IEEE 11th International Conference on Computer Vision, ICCV 2007* 1-8 (2007)
9. Bianco, S., Gasparini, F., and Schettini, R., "Consensus-based framework for illuminant chromaticity estimation," *Journal of Electronic Imaging* 17/(2) 023013 Apr-Jun (2008)
10. Gijssenij, A. and Gevers, T., "Color Constancy using Image Regions," *IEEE International Conference on Image Processing. ICIP 2007. III* 501-504. (2007)
11. Land, E.H., and McCann, J. "Lightness and Retinex theory," *J. of the Optical Soc. of America*, 61 (1) (1971).
12. Ogata, M., Tsuchiya, T., Kubozono, T., and Ueda, K., "Dynamic range compression based on illumination compensation", *IEEE Trans. on Consumer Electronics* 47, (3) (2001)
13. Jobson, D.J., Rahman, Z and Woodell, G.A., "Properties and performance of a CenteriSurrond Retinex", *IEEE Trans. on Image Process.*, 6(3) (1997).

14. [Marsi, S.; Impoco, G.; Ukovich, A.; Ramponi, G.; Carrato, S., "Using a Recursive Rational Filter to Enhance Color Images" IEEE Transactions on Instrumentation and Measurement 57\(6\) 1230-1236 \(2008\).](#)
15. [Saponara, S.; Fanucci, L.; Marsi, S.; Ramponi, G.; Kammler, D.; Witte, E.M., "Application-Specific Instruction-Set Processor for Retinex-Like Image and Video Processing" IEEE Transactions on Circuits and Systems II: Express Briefs, 54\(7\) 596-600 \(2007\)](#)
16. [Meylan, L.; Susstrunk, S., "High dynamic range image rendering with a retinex-based adaptive filter," IEEE Transactions on Image Processing 15\(9\) 2820-2830 \(2006\).](#)
17. [Meylan, L., Alleysson, D., and Susstrunk, S., "A Model of Retinal Local Adaptation for the Tone Mapping of Color Filter Array Images," Journal of the Optical Society of America A \(JOSA A\), 24 \(9\) 2807-2816 \(2007\).](#)
18. Restrepo A., Marsi, S. and Ramponi, G. 'HSV Domain Enhancement of High Contrast Images'. VISAPP09 February, 2009, Lisbon, Portugal. (2009)
19. [Restrepo, A., Rodriguez, C. and Vejarano, C., "Circular Processing of the hue variable: a Particular Trait of Colour Image Processing," VISSAP Second International Conference On Computer Vision Theory and Applications, Barcelona, Spain . \(2007\)](#)
20. Restrepo, A., Marsim S and Ramponi, G., "Chromatic enhancement for virtual restoration of art works". EVA 08, Florence, V. Cappellini and J. Hemsley, eds. Pitagora, Bologna, 94-99 (2008).
21. [Wyszecki, G. and Stiles, W.S., \[Color Science: Concepts and Methods, Quantitative Data and Formulae\] Wiley, New York \(1982\).](#)
22. [Smith, A.R., "Color gamut transform pairs," SIGGRAPH'78, Conf. Procs. Computer Graphics 12\(3\) 12-19 \(1978\).](#)
23. [Kehtarnavaz, N., Kim, N., and Gamadia, M., "Real-time auto white balancing using DWT-based multi-scale clustering", Procs. SPIE 6063 74-82 \(2006\).](#)
24. [Gasparini, F., and Schettini, R., "Color correction for digital photographs," Procs. 12th Int. Conf. on Image Analysis and Processing, Mantova, Italy, pp. 646-651 \(2003\).](#)
25. [Lam, E.Y., "Combining gray world and retinex theory for automatic white balance in digital photography," Procs. 9th Int. Symp. on Consumer Electronics, Macau, Hong Kong, 134-139 \(2005\)](#)
26. [R. Lukac. 'Refined automatic white balancing.' ELECTRONICS LETTERS, 43\(8\) \(2003\)](#)
27. [C. Tomasi and R. Manduchi., 'Bilateral filtering for gray and color images'. IEEE Int. Conf. Computer Vision, Bombay, India. \(1998\)](#)